First Physics Results from RHIC with An Introduction to the Physics of Relativistic Heavy Ion Collisions— The Search for the Quark-Gluon Plasma: A New State of Matter

M. J. TANNENBAUM
Brookhaven National Laboratory
Upton, NY 11973-5000 USA
E-mail:mjt@bnl.gov

A summary of measurements from the first year's run at RHIC will be presented. The second year's run at RHIC is presently underway with Au+Au (300 μb^{-1}) and p-p (3.5 pb^{-1}) collisions planned at $\sqrt{s_{NN}} = 200$ GeV.

Quantum Chromodynamics, the theory of strong interactions, predicts the transition of hot dense nuclear matter to a state of deconfined quarks and gluons in thermal and chemical equilibrium over a significant volume (a 10fm[10×10^{-13} cm] cube). Signatures of this proposed new state of matter will be discussed in the light of present measurements and future prospects.

Colloquium, UConn, November 16, 2001

High Energy Nucleus-Nucleus Collisions

♡ High Energy Nucleus-Nucleus Collisions provide the means of creating Nuclear Matter in conditions of Extreme Temperature and density

♡ At large energy densities or Baryon Density, a Phase Transition is expected from a state of nucleons containing confined quarks and gluons to a state of “deconfined” (from their individual nucleons) quarks and gluons covering the entire volume of nuclear matter, or a volume that is many units of the characteristic interaction length scale:

$$\Lambda_{\rm QCD}^{-1} \sim (0.1GeV)^{-1} \sim 2\,fm$$

♡ This state should be in Chemical and Thermal Equilibrium

♡ This is the Quark Gluon Plasma (QGP)

The Major Questions in the Field Are:

♡ How to relate the thermodynamical properties, Temperature (T), energy density (ϵ), entropy (S) . . . of the QGP or hot nuclear matter to properties that can be measured in the laboratory.

♡ How to detect when/if the QGP is produced and to measure its properties.

E. O'Brien - RHIC2000

The Relativistic Heavy Ion Collider at BNL

- Two independent rings 3.83 k in circumference
  - 120 bunches/ring
  - 106 ns crossing time
- Maximum Energy
  - $s^{½}$ = 500 GeV p-p
  - $s^{½}$ = 200 GeV Au-Au per N-N collision
- Design Luminosity
  - Au-Au $2\mathrm{x}10^{26}\ \mathrm{cm}^{-2}\mathrm{s}^{-1}$
  - p - p $2\mathrm{x}10^{32}\ \mathrm{cm}^{-2}\mathrm{s}^{-1}$ (polarized)
- Capable of colliding any nuclear species on any other nuclear species

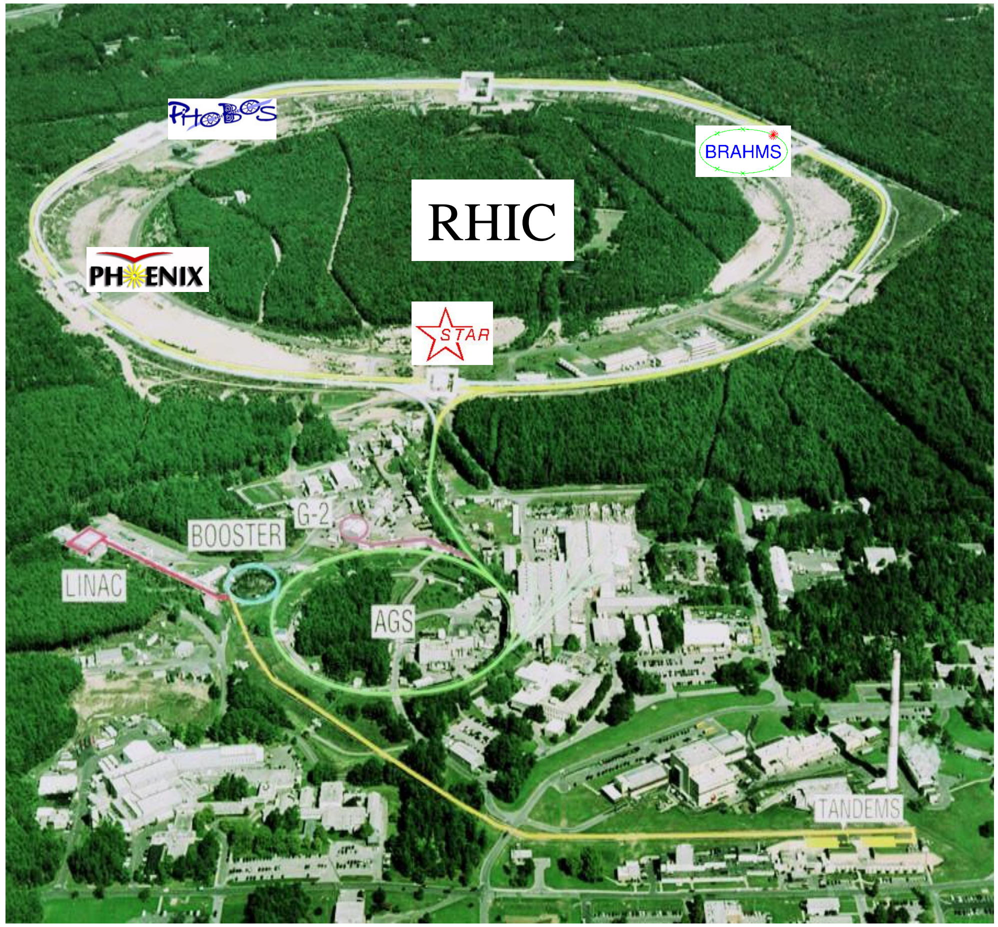

RHIC Experiments at a Glance

- **PHENIX**
  - High Granularity, High Resolution Central Spectrometer for electrons, photons and charged hadrons, $|\eta| < 0.35$, $\Delta\Phi = \pi$
  - Electron ID at the trigger level with RICH, EMCal, tracking
  - high segmentation $\gamma - \pi^0$ separation for $p_T \leq 25$ GeV/c
  - Two Endcap Di-Muon Spectrometers $1.1 \leq |y| \leq 2.5$
  - study of J/Ψ Ψ' via e^+e^-, $\mu^+\mu^-$
- **STAR**
  - large acceptance TPC tracking detector
  - good PID for $p_T \leq 1$GeV/c
  - central TPC full tracking in $\Delta\Phi = 2\pi$ $|\eta| < 1$
  - endcap TPC extends tracking to $|\eta| \leq 2$
  - upgrade to Barrel/Endcap EMCalorimeter $|\eta| \leq 1 - 2$
  - Silicon Vertex Detector for short lived hyperons
- **PHOBOS**
  - large area silicon tracking ($dN_{ch}/d\eta$ over 4π)
  - momentum and particle ID at midrapidity $p^\pm$, $K^\pm$, $\pi^\pm$
  - interested in long lived sources, HBT at very low p_T
- **BRAHMS**
  - moveable 2-arm spectrometer
  - small solid angles, excellent PID
  - $p^\pm$, $K^\pm$, $\pi^\pm$ over wide kinematic and rapidity range

Our First Event, June 12, 2000

Au+Au $\sqrt{s_{NN}} = 56$ GeV

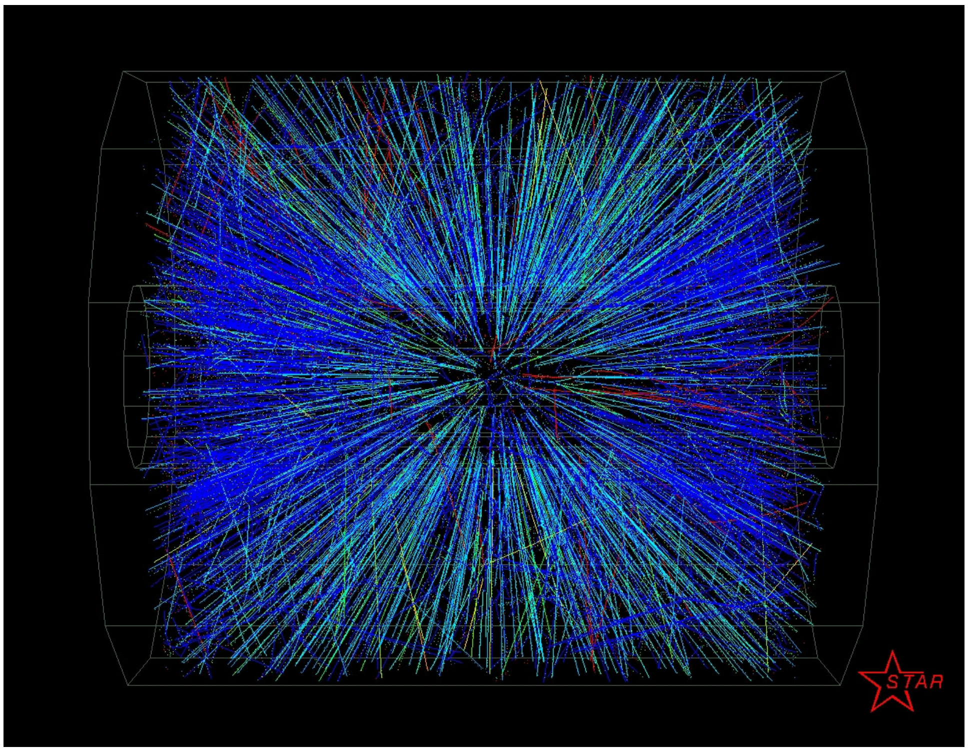

STAR—l'Étoile

Typical Variables Used

• **Longitudinal and Transverse momentum:** For any particle, the momentum is resolved into transverse (p_T) and longitudinal (p_L) components; and in many cases the mass (m) of the particle can be determined.

• **Rapidity and Transverse mass:** Rapidity is used for the longitudinal component since it transforms linearly under a Lorentz transformation

$$y = \ln\left(\frac{E + p_L}{m_T}\right)$$

where

$$m_T = \sqrt{m^2 + p_T^2} \quad \text{and} \quad E = \sqrt{p_L^2 + m_T^2}$$

• **Pseudorapidity:**

In the limit $m \ll E$ the rapidity reduces to the pseudorapidity(η)

$$\eta = -\ln\tan\theta/2$$

• **Invariant Cross Section** The Lorentz invariant differential single particle inclusive cross section is:

$$\frac{Ed^3\sigma}{dp^3} = \frac{d^3\sigma}{p_T dp_T dy d\phi} \qquad \text{where} \quad dy = \frac{dp_L}{E}$$

• **Beam Rapidity and Mid-Rapidity**

$$Y_{\rm Beam} = \ln\left(\frac{p + \sqrt{p^2 + M_{\rm N}^2}}{M_{\rm N}}\right) \qquad y_{\rm NN} = Y_{\rm Beam}/2$$

Typical Quantities Measured and Their Interpretation

• **Temperature (T) :**

$$< p_T > \sim \; T$$

• **Entropy (S) :** The number of particles n produced on a collision, the multiplicity, is taken as proportional to the entropy.

• ***dn/dy* :** dn/dy the multiplicity density in rapidity is the most commonly used variable

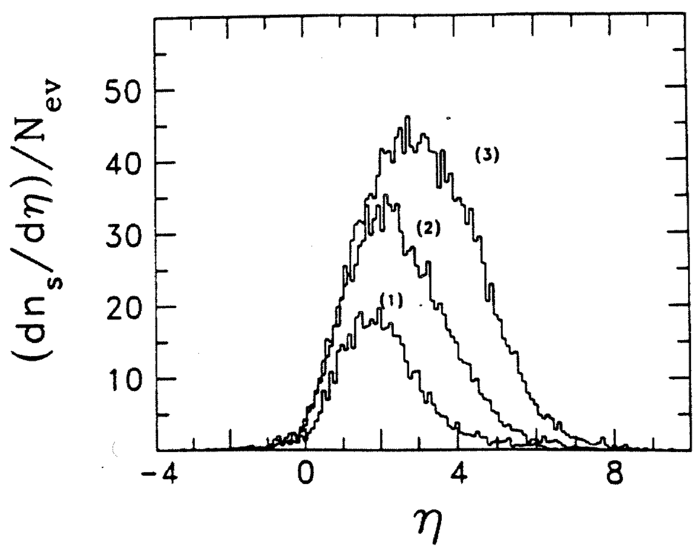

Figure 1: $dn/d\eta$ of relativistic particles for ^{16}O+AgBr Central Collisions. (1) 14.6 GeV/c, (2) 60, (3) 200 GeV/nucleon

• **Comoving Energy Density (ϵ) :**

$$< p_T > \times dn/dy \equiv dE_T/dy \sim \epsilon$$

According to Bjorken, this measures the spatial energy density.

Nuclear Geometry Definition—Experiment

Identical Zero Degree Calorimeter all Expts

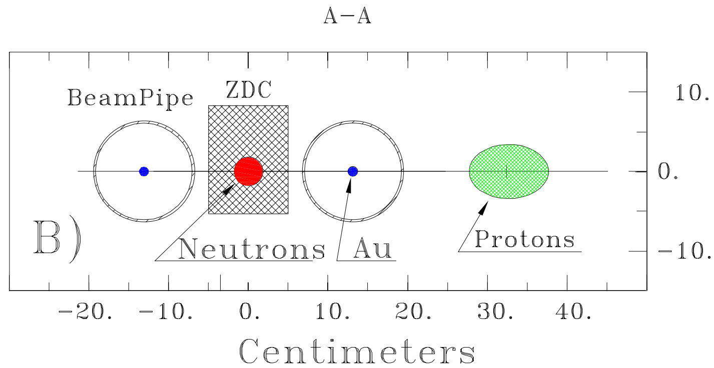

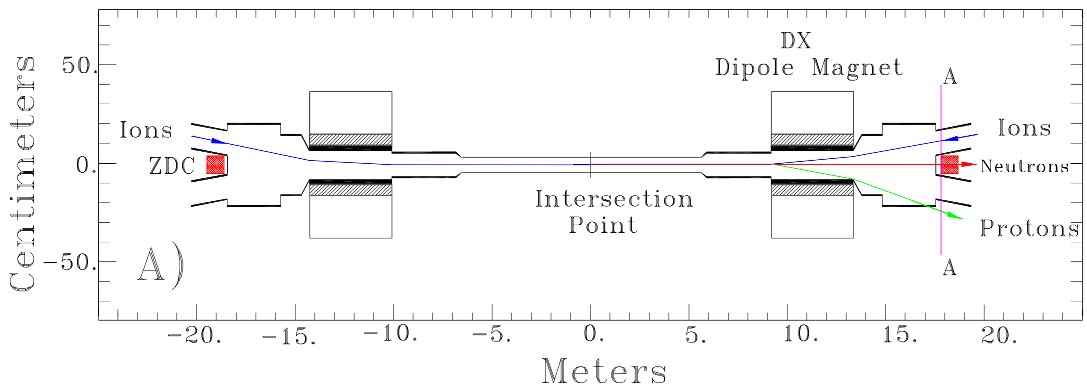

Plus/or BeamBeam/Paddle Counters $3 \leq |\eta| \leq\sim 4$

Phenix Ideal

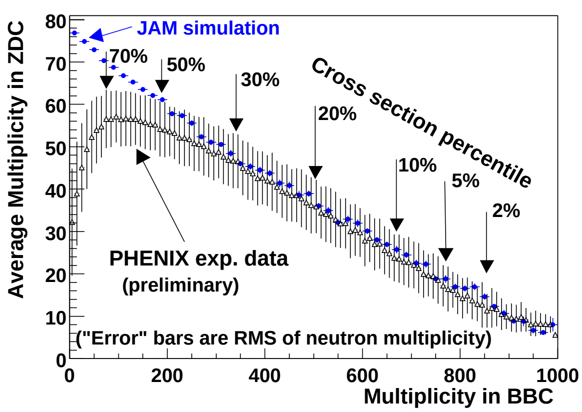

Phenix Real

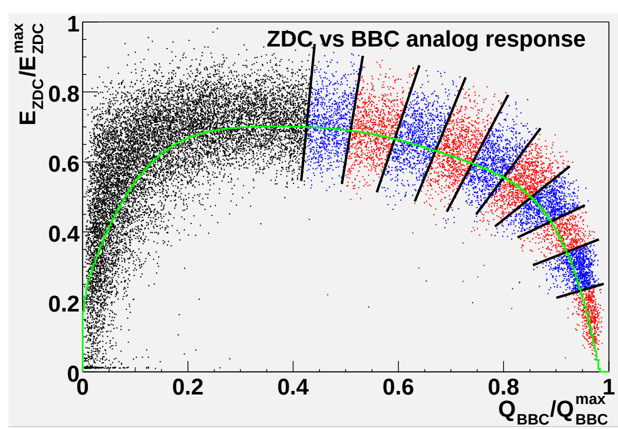

Schematic Nuclear Collision Geometry

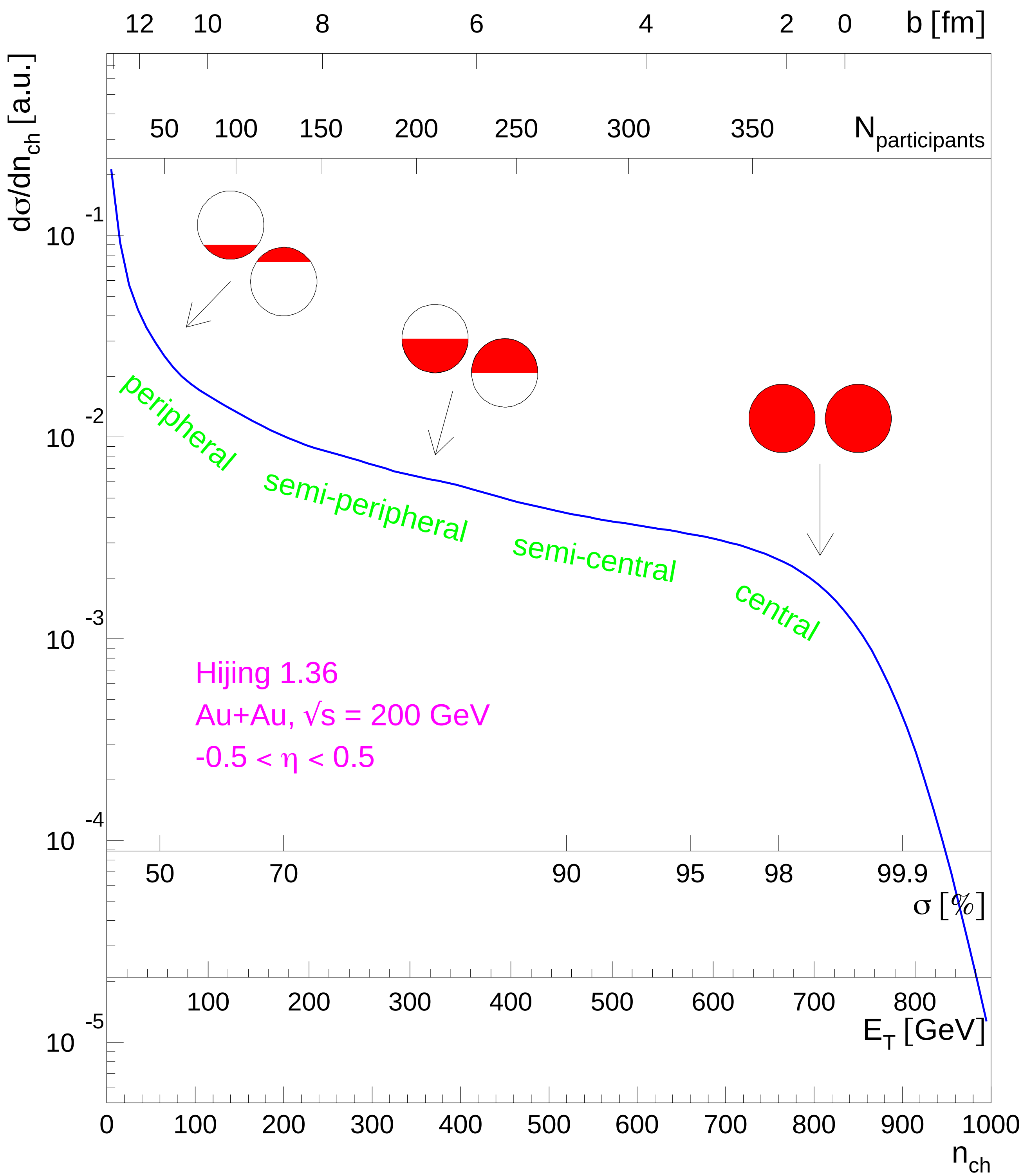

Figure 2: Schematic Nuclear Collision Geometry from Star-Yale

Real E_T Distributions—from AGS

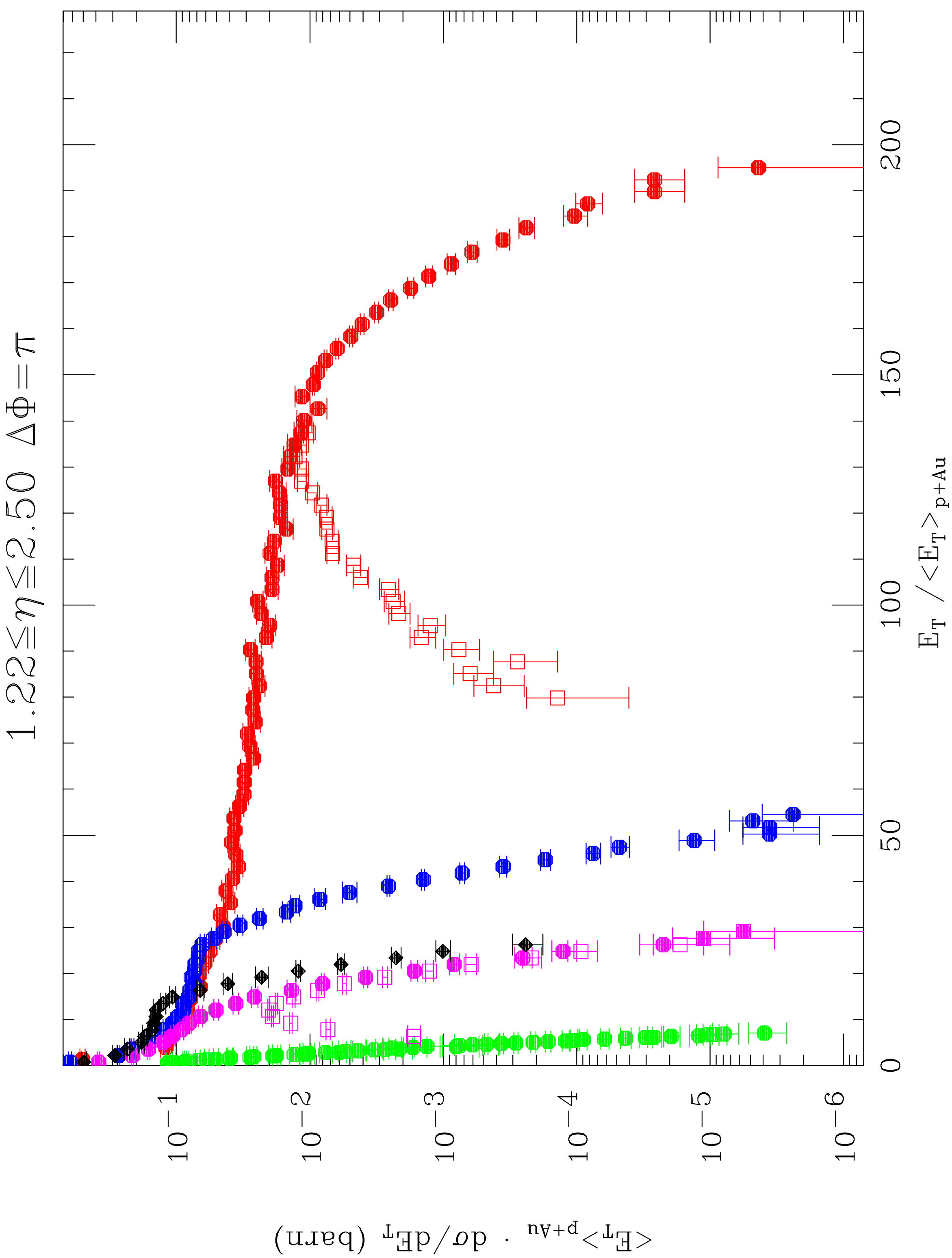

First RHIC Publication 19 July 2000

Phobos $dN_{ch}/d\eta|_{|\eta|<1}$

Phys. Rev. Lett. 85, 3100 (2000), nucl-ex/0108009

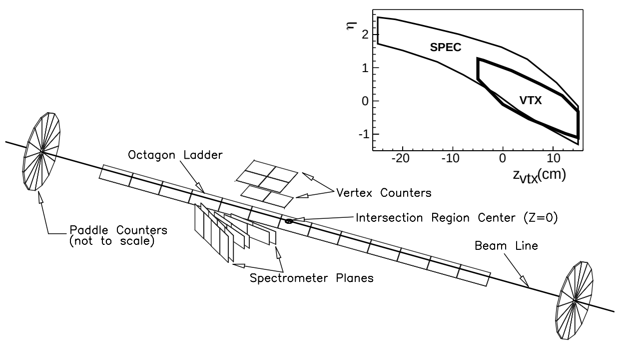

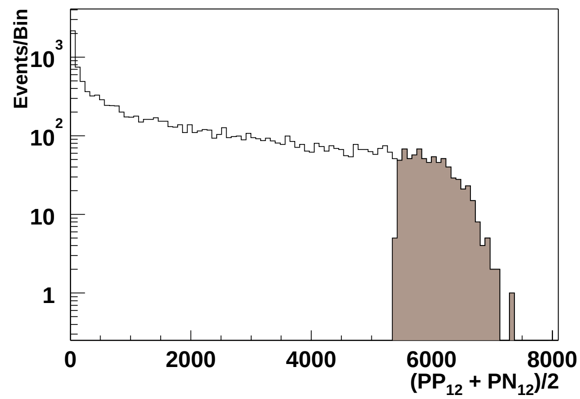

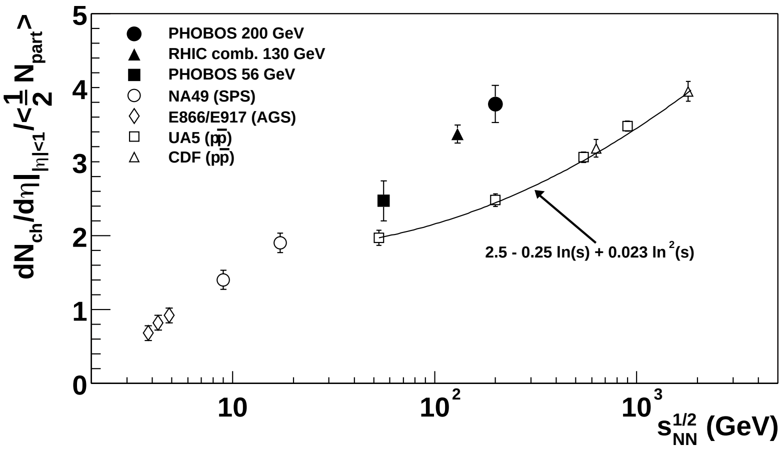

Figure 3: central (top 5.4%) $dN/d\eta$ per participant pair cf p-p

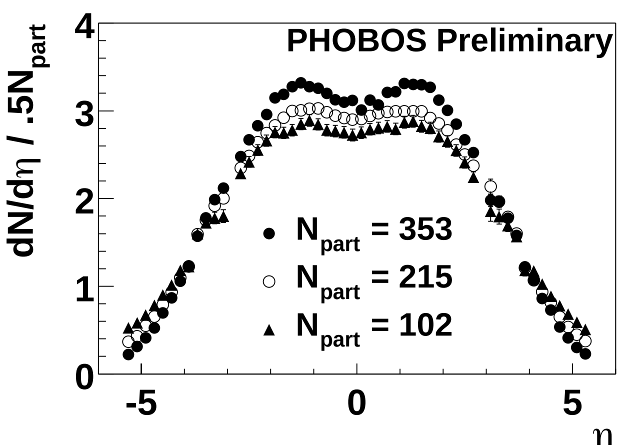

Figure 4: $dN/d\eta$ per participant pair vs η

PHENIX $dN_{ch}/d\eta|_{\eta=0}$ $dE_T/d\eta|_{\eta=0}$

Phys. Rev. Lett. **86**, 3500 (2001),Phys. Rev. Lett. **87**, 052301 (2001)

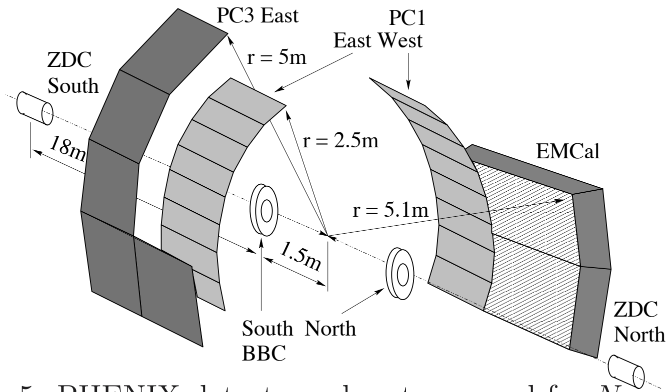

Figure 5: PHENIX detector subsystems used for N_{ch}, E_T, π^0

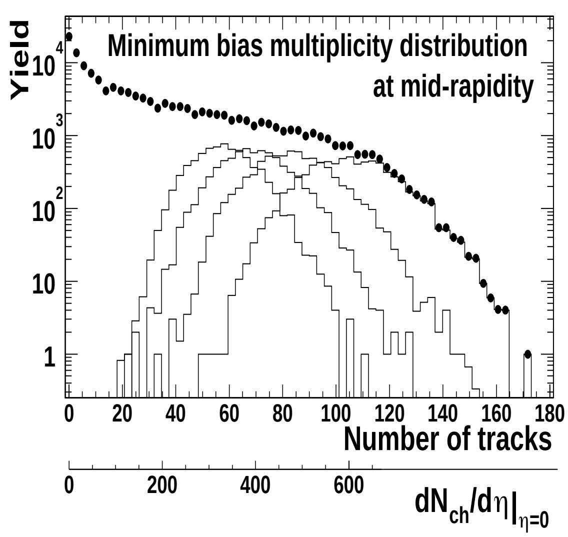

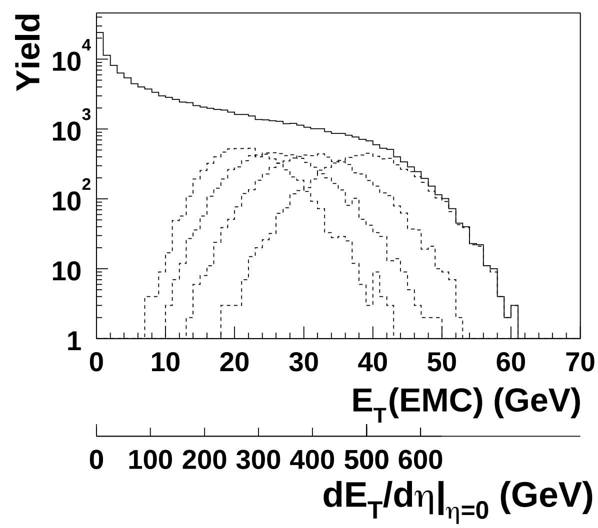

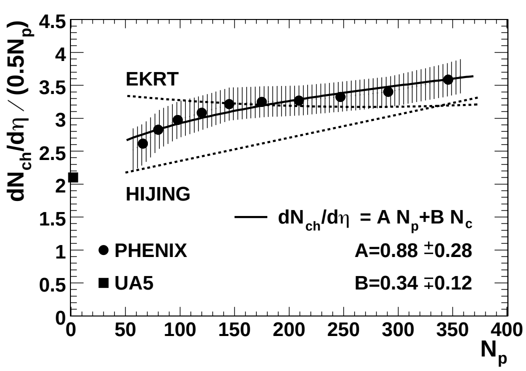

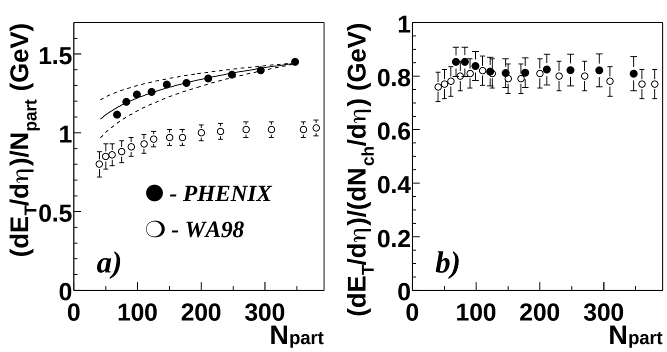

WNM fails, term $\propto N_{coll}$ indicated

$\epsilon_{Bj} = \frac{dE_T}{dy}\frac{1}{\pi R^2} \rightarrow 4.6$ **GeV/fm^3 at RHIC (top 2%) cf 2.9 CERN**

due to increase in multiplicity $\langle E_T\rangle/\langle N_{ch}\rangle$ stays constant

Shape of Upper Edge is Acceptance Dependent

<u>Acceptance cut in E_t measurements</u>

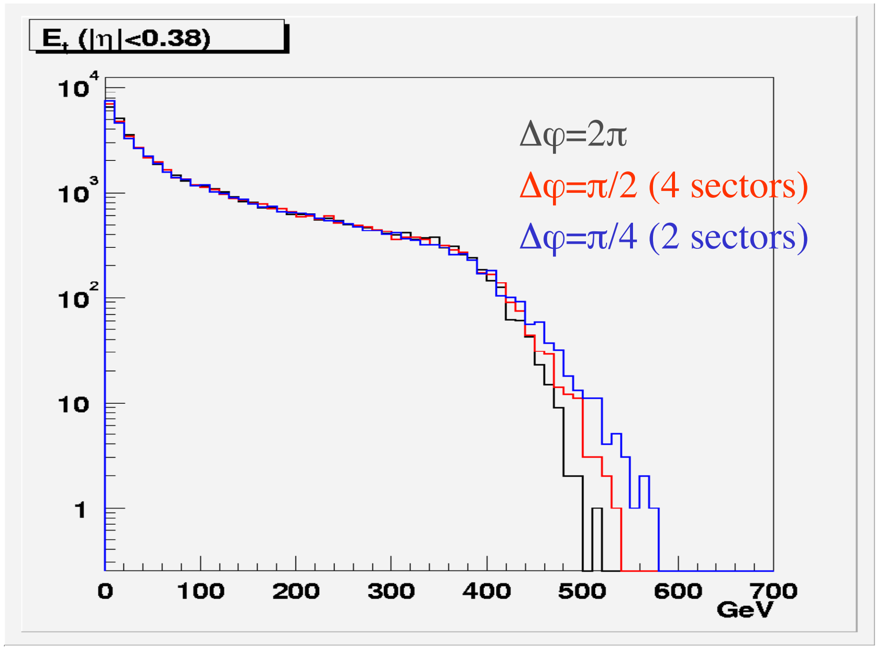

Limited EMCal acceptance changes *Et* distribution tail due to fluctuations of the number of particles in acceptance

Signatures of the Quark Gluon Plasma

- **Characteristic Temperature Entropy Curve :**

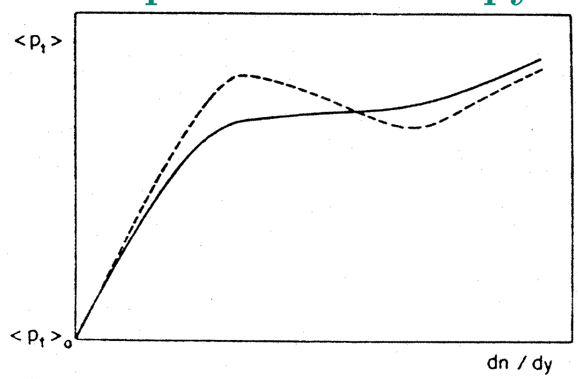

Note that this curve has the features of a phase transition with which we are all familiar. The $< p_T >$, acting as temperature, increases with increasing entropy (dn/dy); then as the phase transition takes place (e.g. water changing to steam) the temperature remains constant and begins rising again when the transition to the new phase is complete.

- **Plasma Droplets caused by Deflagration :** These would be manifested by large fluctuations in dn/dy or dE_T/dy covering a range of $\sim$1 unit on an event by event basis. The hope would be to observe the other plasma signatures only in the region of the fluctuation and not in the other regions.

- **Thermal Equilibrium :** Characteristic Thermal production should be exhibited. For a thermal distribution:

$$d^3n/dp^3 = G(\theta)\frac{C}{e^{(E-\mu)/T} \pm 1}$$

where the + sign is for particles which obey Fermi-Dirac statistics and the - sign for Bose-Einstein statistics. $G(\theta)$ is the angular distribution, C is a constant and μ is called the chemical potential. At each rapidity y, $E = m_T \cosh y$, so we get

$$E\, d^3n/dp^3 \simeq G(y)\, m_T\, e^{-m_T/T_B(y)}$$

$\Rightarrow$ For a true thermal distribution the dependence is only on $m_T = \sqrt{p_T^2 + m^2}$ for particles of different masses.

• **Thermal Photon/Lepton-Pair Emission :** Photons emitted in the QGP will come out without further interacting (they don't strongly interact) so they give information on the temperature T_c of the phase transition:

$$\frac{dN_\gamma/dy}{[dn/dy]^2} \propto T_c$$

• **Chemical Equilibrium :**

In the QGP there will be gluons, quarks and anti-quarks. They will continuously react with each other via the QCD subprocesses:

$$g\,g \to q\,\bar{q} \qquad q\,\bar{q} \to g\,g \qquad q\,q \to q'\,q'$$

where q' represents a different flavor quark (u, d or s).

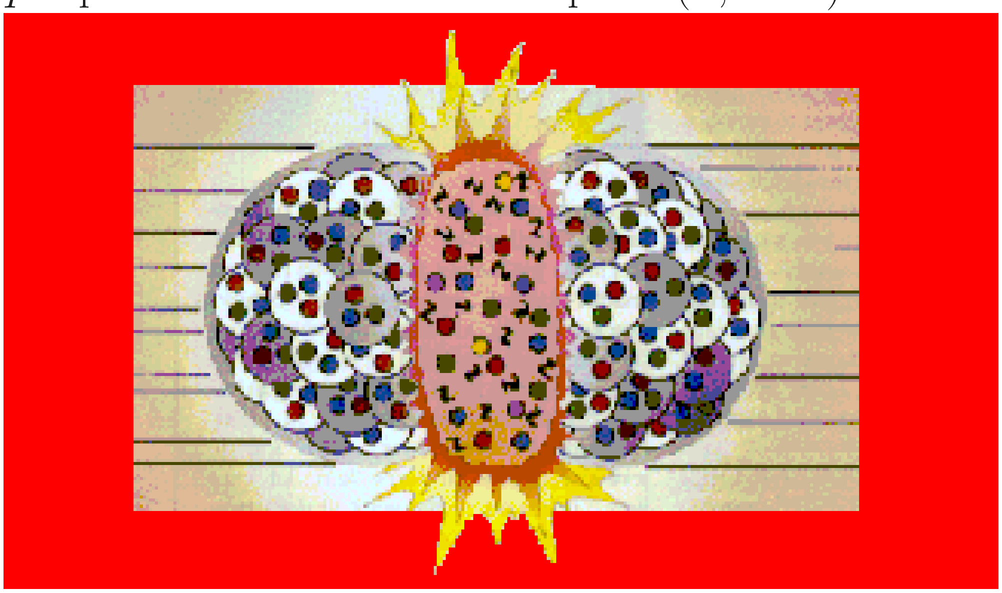

After several interactions have taken place, the reaction rates and the abundances of the gluons and the different flavor quarks (and anti-quarks) will become equilibrated, so that they no longer change with time. This is called chemical equilibrium. Since the transition temperature T_c is comparable to the strange quark mass ~150 MeV, the strange quarks $s, \bar{s}$ should have the same abundance as the $u, \bar{u}$

and $d, \bar{d}$ in the QGP.

$\Rightarrow$ Particle Composition Should Be different in QGP than a hadron gas or 'ordinary' $p-p$ or $A-A$ reactions

$$\frac{K^-(s\bar{u})}{\pi^-(d\bar{u})} \qquad \frac{K^+(u\bar{s})}{\pi^+(u\bar{d})}$$

• **Deconfinement :** J/Ψ production in the $A-A$ collision is suppressed by the Debye Screening of the Quark Color charge in the Plasma.

The plasma deconfines the $c\bar{c}$ in the J/Ψ by Debye Screening. The c and $\bar{c}$ later pick up other quarks to become charm particles.

• **Other Medium Effects :** The QGP may restore the spontaneously broken symmetry of the Vacuum leading to 'Disordered Chiral Condensates' or Chiral Symmetry Restoration (particle masses change). Quarks and gluons will lose/transfer energy in the medium...

High p_T Physics

From a talk I gave in 1998

My Best Bet on Discovering QGP
Utilizes semi-Inclusive π^0 or $\pi^\pm$ production

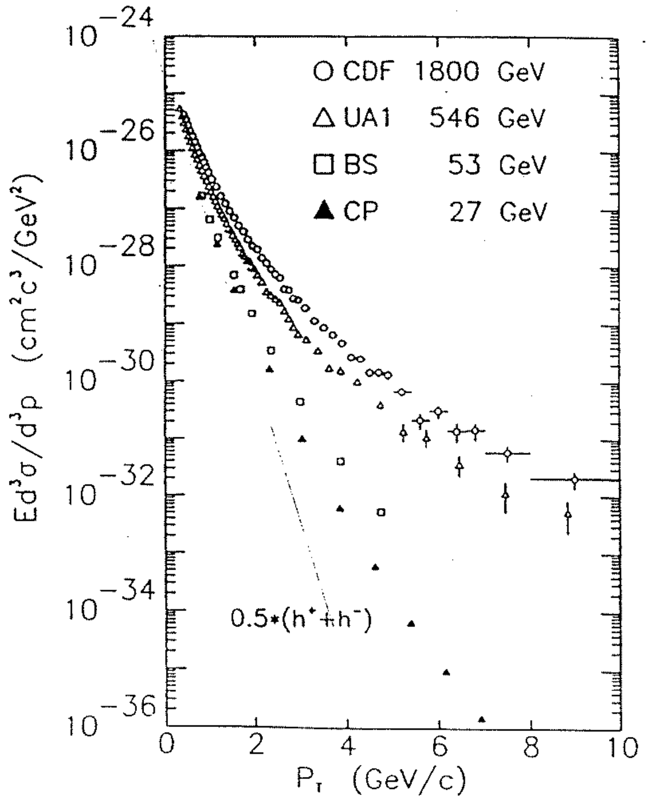

Invariant cross section for non-identified charged-averaged hadron production at 90° in the c.m. system as a function of the transverse momentum p_T tablulated by CDF for a range of C.M. energies $\sqrt{s}$. There is an exponential tail (e^{-6p_T}) at low p_T, which depends very little on $\sqrt{s}$. This is the soft physics region, where the hadrons are fragments of 'beam jets'. At higher p_T there is a power-law tail which depends very strongly on $\sqrt{s}$. This is the hard-scattering region, where the hadrons are fragments of the high p_T QCD jets from constituent-scattering. **My hope is that the QGP causes the high p_T quarks to lose all their energy and stop, so that the high p_T tail will 'vanish' for central Au+Au collisions**

In RHI central collisions, leading particles are the only way to find jets because in one unit of Δr there is $\pi \times \frac{1}{2\pi}\frac{dE_T}{d\eta} \sim 375$ GeV !!!.

Experimental Probes of the QGP

• **Collision Geometry :** is determined from charged particle multiplicity, dn/dy, and Transverse Energy Flow, dE_T/dy

♡ **Comoving Energy Density :** is also determined by dE_T/dy

♡ **Entropy :** is also determined by dn/dy

• **Yields and m_T distributions :** of identified hadrons of various species give information on Freezout Temperature ($<p_T>$), and possible Chemical Equilibrium and Thermal Equilibrium

• **Single Photons and Lepton Pairs :** are penetrating probes from the early stage of the collision and their yields are sensitive to the initial temperature and the time evolution of the system

• **J/Ψ suppression :** probes deconfinement, a key feature of a Quark Gluon Plasma

• **Net Baryon Density :** is probed by the rapidity distribution of the nucleons

• **Hanbury-Brown Twiss Effect :** The Quantum Mechanical interference due to symmetry (Bose) or antisymmetry (Fermi) of the wave function of 2 (or more) identical particles e.g. $K^+ K^+$ is sensitive to the dimensions of the system at freezeout ...

• **Dense Medium Effects :**

♡ **Mass Shifts :**

♡ **Jet Quenching at large p_T :** ...

PHENIX Identified Hadrons

It's a real effect—different from $p-p$

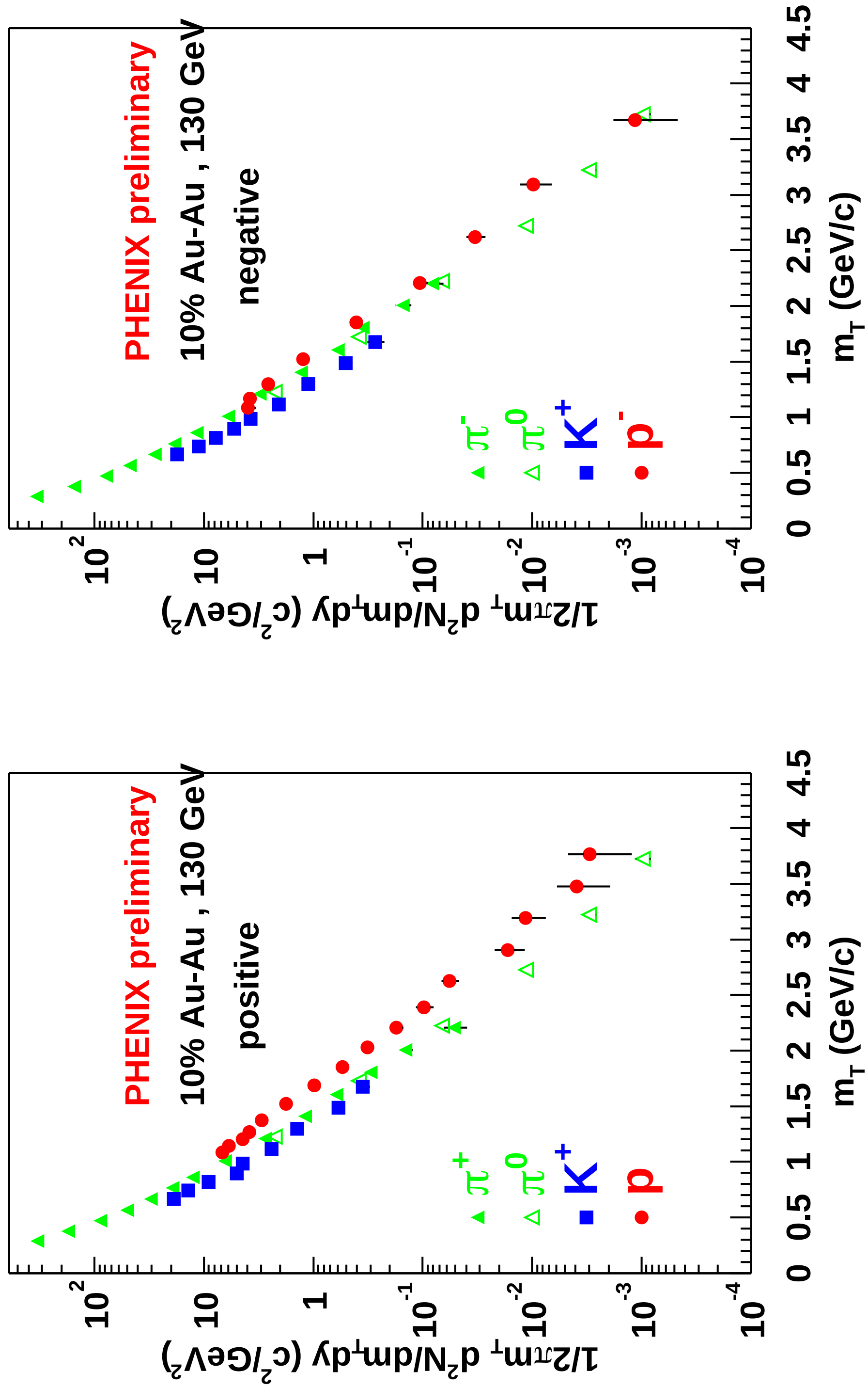

protons dominate pions for $p_T \geq 2$ GeV/c !!!

Identified $\pi^{\pm}$, $K^{\pm}$ $p^{\pm}$

PHENIX—QM2001 Proceedings

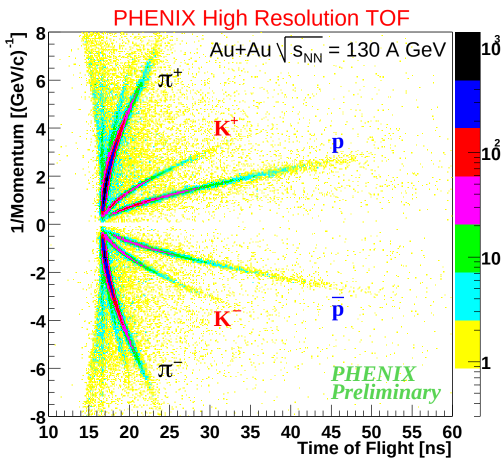

Figure 6: PHENIX PID in Time of Flight $|\eta| \leq 0.35$ $\Delta\Phi = \pi/8$

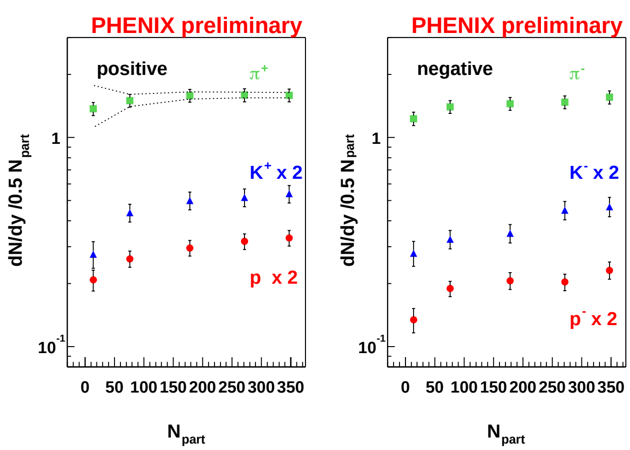

Figure 7: Identified Charged Particles vs Centrality

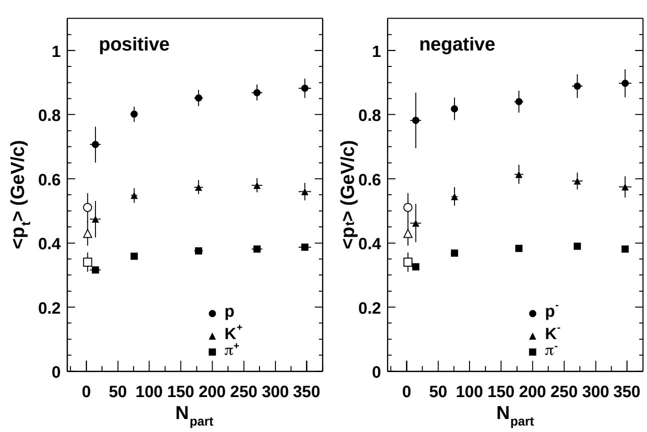

Figure 8: $\langle p_T \rangle$ vs N_{part} (dn/dy). Where is VanHove Signature?

$\bar{p}/p$, K^-/K^+, π^-/π^+

All 4 Experiments Agree

Little or No dependence on centrality or p_T

		$\bar{p}/p$	MidRapidity
STAR (PRL **86**)	MinBias	$0.65 \pm 0.01 \pm 0.07$	$0.4 \leq p_T \leq 1.0$ GeV/c
PHENIX	MinBias	$0.64 \pm 0.01 \pm 0.07$	$0.8 \leq p_T \leq 3.0$ GeV/c
PHOBOS	top 11%	$0.60 \pm 0.04 \pm 0.06$	$0.1 \leq p_T \leq 1.0$ GeV/c
BRAHMS	top 40%	$0.62 \pm 0.04 \pm 0.05$	$0.4 \leq p_T \leq 1.9$ GeV/c

		K^-/K^+	MidRapidity
PHENIX	MinBias	$0.92 \pm 0.03 \pm 0.22$	$0.8 \leq p_T \leq 1.6$ GeV/c
PHOBOS	top 11%	$0.91 \pm 0.07 \pm 0.06$	$0.1 \leq p_T \leq 0.7$ GeV/c
BRAHMS	top 40%	$0.89 \pm 0.07 \pm 0.05$	$0.3 \leq p_T \leq 1.7$ GeV/c

		π^-/π^+	MidRapidity
PHOBOS	top 11%	$1.00 \pm 0.01 \pm 0.02$	$0.2 \leq p_T \leq 0.6$ GeV/c
BRAHMS	top 40%	$0.95 \pm 0.03 \pm 0.05$	$0.3 \leq p_T \leq 1.7$ GeV/c

Brahms—y dependence of $\bar{p}/p$

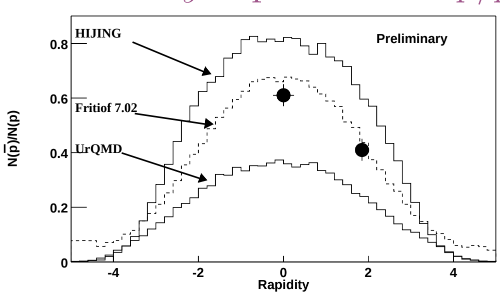

$\sqrt{s_{NN}}$ Dependence

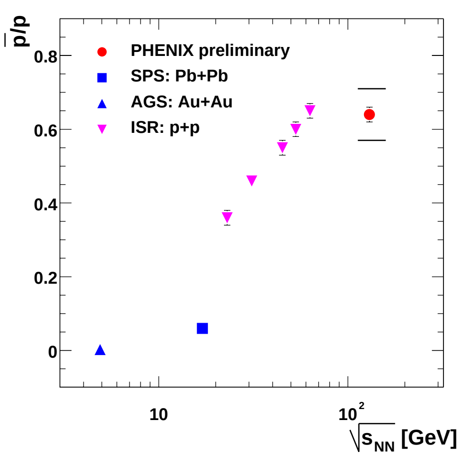

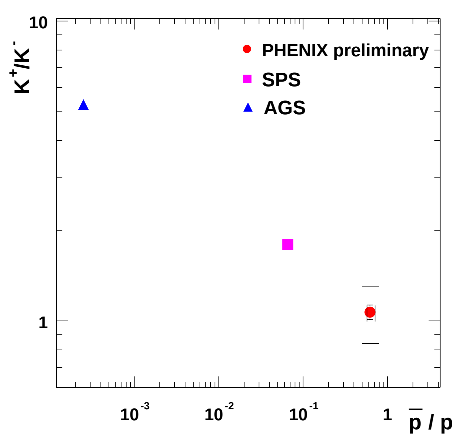

Hard Scattering is Point-Like
From DIS

E. Gabathuler, Total cross-section

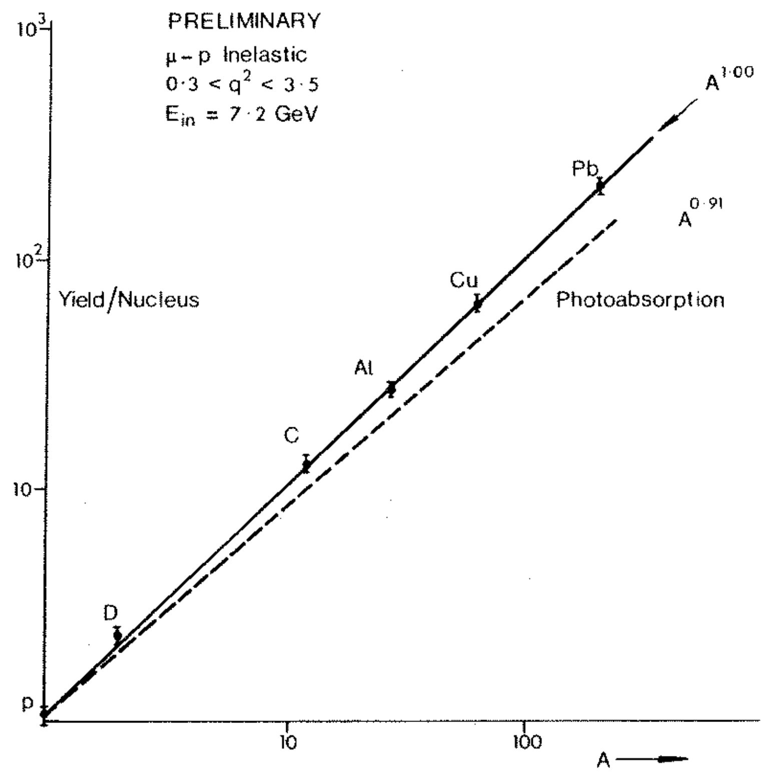

Fig. 14. The *A* dependence of the inelastic muon cross-section as presented by Tannenbaum (see discussion).

AGS $\mu - A$ scattering data, from E. Gabathuler's talk, [Proc. 6th Int. Symposium on Electron and Photon Interactions at High Energies, Bonn (1973)].

♡ DIS is pointlike $A^{1.00}$ even at modest q^2—no shadowing.
♡ Photoproduction is shadowed—$A^{0.91}$

High p_T in A+B—T_{AB} Scaling

Hard-scattering is a point-like process, with excellent PQCD predictions $\sim 10\%$ for $p-p$ and $\bar{p}-p$ collisions. For p+A or A+A collisions the cross sections should scale by the number of point sources, A for p+A or A^2 for A+A.

As a function of impact parameter, the profile function for a nucleus A

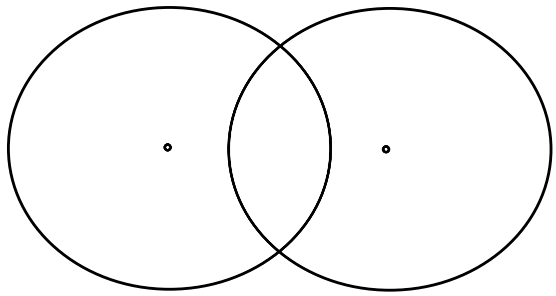

$$T_A(\vec{s}) = \int dz \rho_A(z, \vec{s})$$

is the number of nucleons per unit area along a direction z at a point from the center of the nucleus represented by a 2-d vector $\vec{s}$, where z is perpendicular to $\vec{s}$. For an interaction of nucleus A with nucleus B at impact parameter $\vec{b}$, the nuclear overlap integral $T_{AB}(\vec{b})$ is defined:

$$T_{AB}(\vec{b}) = \int d^2 s T_A(\vec{s}) T_B(\vec{b} - \vec{s}) \quad ,$$

where $d^2s = 2\pi s ds$ is the 2-dimensional area element. Simply:

$$T_{AB}(\vec{b}) = N_{coll}(\vec{b}, \sigma)/\sigma$$

More precisely, for a certain fraction f of the nuclear interaction cross section for A+B collisions, the semi-inclusive yield is related to the $p-p$ inclusive cross section:

$$\frac{1}{N_f} \frac{d^3 N_f^{A+A}}{p_T dp_T dy d\phi} = \frac{d^3 \sigma^{p-p}}{p_T dp_T dy d\phi} \times \langle T_{AB} \rangle_f \cong \frac{d^3 \sigma^{p-p}}{p_T dp_T dy d\phi} \times \frac{\langle N_{coll}(\sigma_{nn}) \rangle_f}{\sigma_{nn}}$$

What Really Happens in Hadron Scattering

The Anomalous Nuclear Enhancement
aka the 'Cronin Effect'
The unpleasant Nuclear Effect

Due to Multiple Scattering of the initial Nucleons (Constituents?)
Now called k_T broadening.
But don't forget 'shadowing' of the Structure Functions in Nuclei
For latest info see E. Wang and X.-N. Wang nucl-th/0104031

CERN Pb+Pb $\sqrt{s_{NN}} = 17.2$ GeV

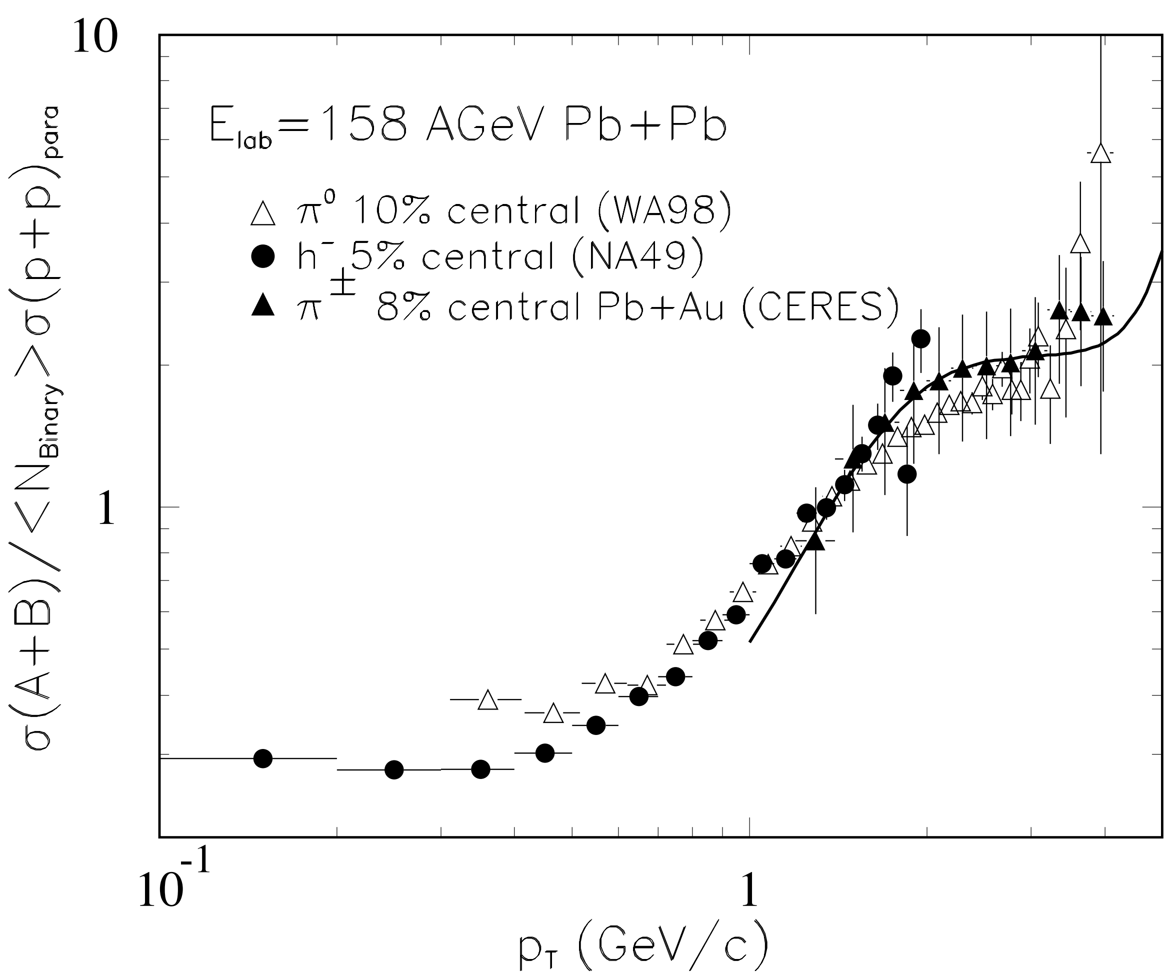

Figure 24: From Wang and Wang nucl-th/0104031

What happens at RHIC—something new! High $p_T \pi^0$ —PHENIX Au+Au $\sqrt{s_{NN}}$=130 GeV

π^0 Cent. and Periph. nucl-ex/0109003

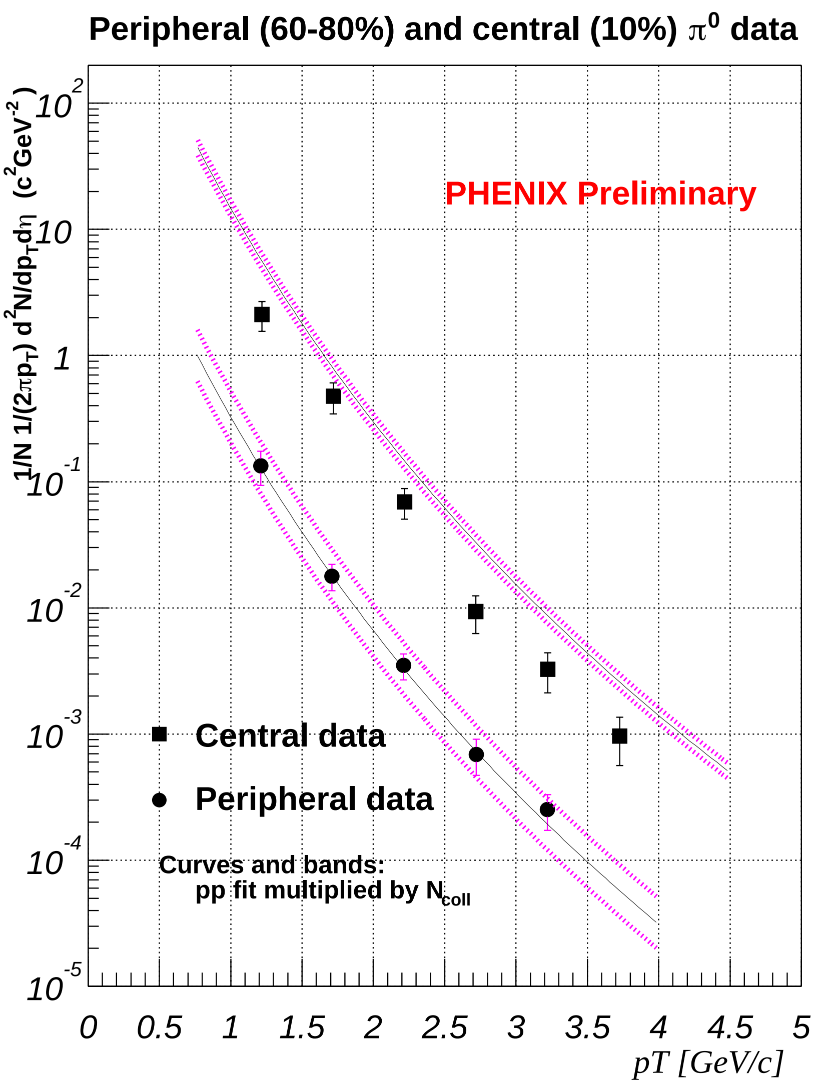

PHENIX central and peripheral π^0 semi-inclusive yield, scaled by $\langle T_{AB} \rangle$ for the centrality class= $\langle N_{coll}(40\text{mb}) \rangle/40\text{mb}$

♡ **Central π^0 yield is BELOW the point-like prediction!!**

A New and Interesting High p_T Nuclear Effect

PHENIX π^0 and $(h^+ + h^-)/2$ Central cf. UA1 fit

A deficit for $p_T > 2$ GeV/c—never seen previously!!!

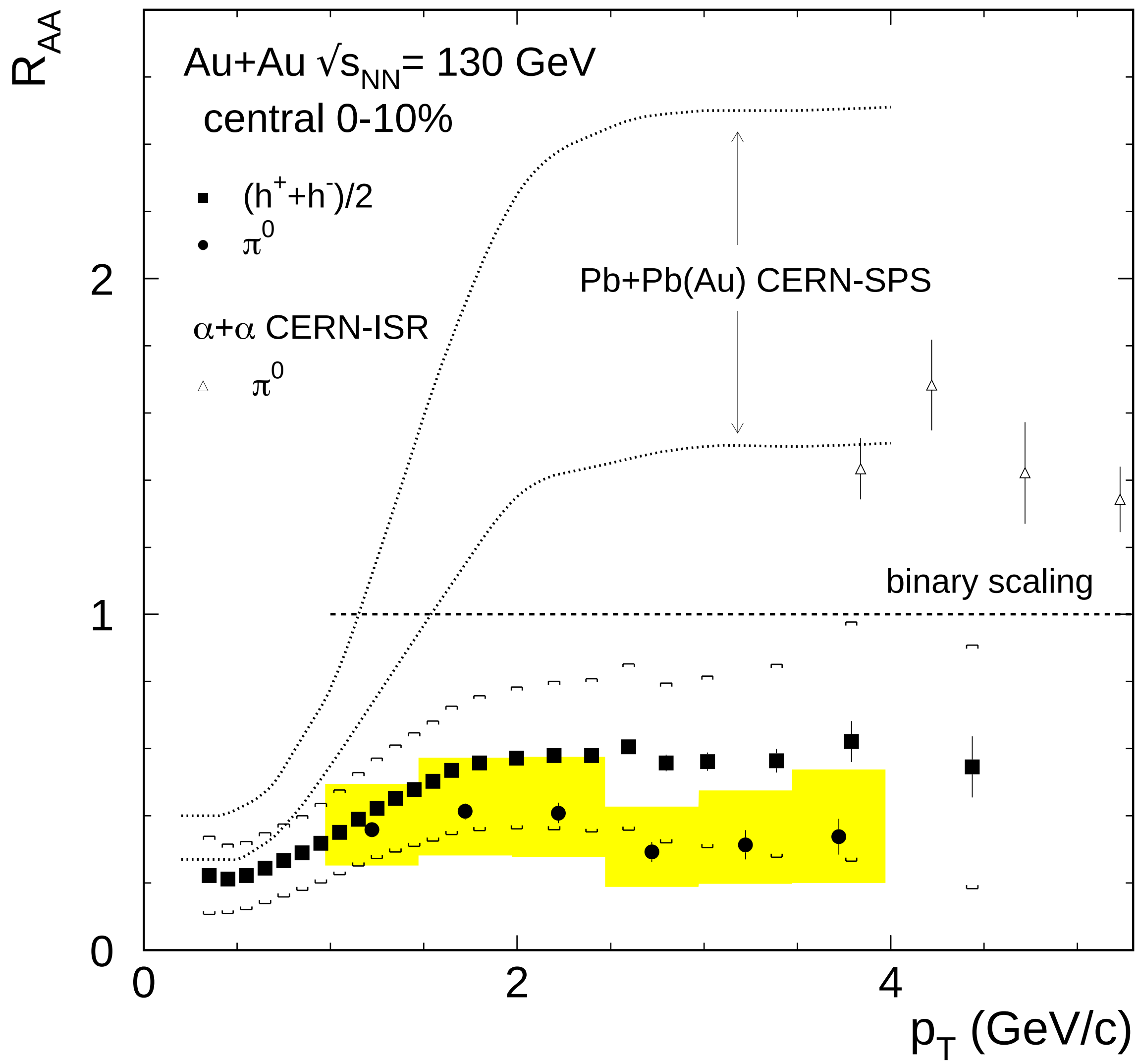

Is this the 'jet quenching' in hot matter predicted by R. Baier, Yu. L. Dokshitzer, A. H. Mueller, S. Peigné and D.Schiff, Nucl. Phys. **B483**, 291 (1997) ?. Too early to say, needs lots more systematic investigation! This year's run at RHIC is presently underway with Au+Au (300 μb^{-1}) and (polarized) p-p (3.5 pb^{-1}) collisions planned at $\sqrt{s_{NN}} = 200$ GeV. Should go to up to $p_T \sim 20$ GeV/c with good p-p comparison if all goes well.

EMCal global energy calibration

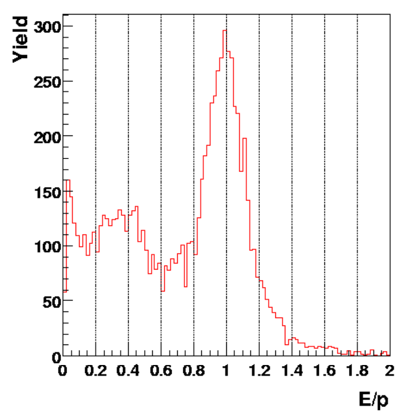

E/p matching
for electron enriched sample (with RICH): p>0.5 GeV/c

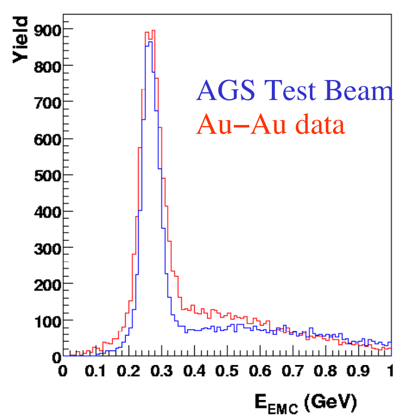

MIP peak position
for 1 GeV/c charged tracks (mostly pions):
Within 2% from Test Beam results

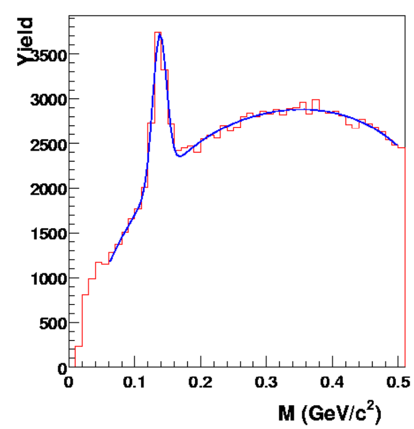

π0's
p_t>2 GeV, asym<0.8

m=136.7±0.3 MeV/c^2

EMCal calibration is consistent within 2%

Event by Event Physics

$$M_{p_T} = \overline{p_T}_{(n)} = \frac{1}{n}\sum_{i=1}^{n} p_{T_i} = \frac{1}{n}E_{Tc}$$

Analytical formula for statistically independent emission

For statistical independent emission an analytical formula for the distribution in M_{p_T} can be obtained. It depends on the 4 semi-inclusive parameters $\langle n \rangle$, $1/k$, b and p which are derived from the quoted means and standard deviations of the semi-inclusive p_T and multiplicity distributions for central Pb+Pb collisions for NA49. The result is in excellent agreement with the NA49 measurement.

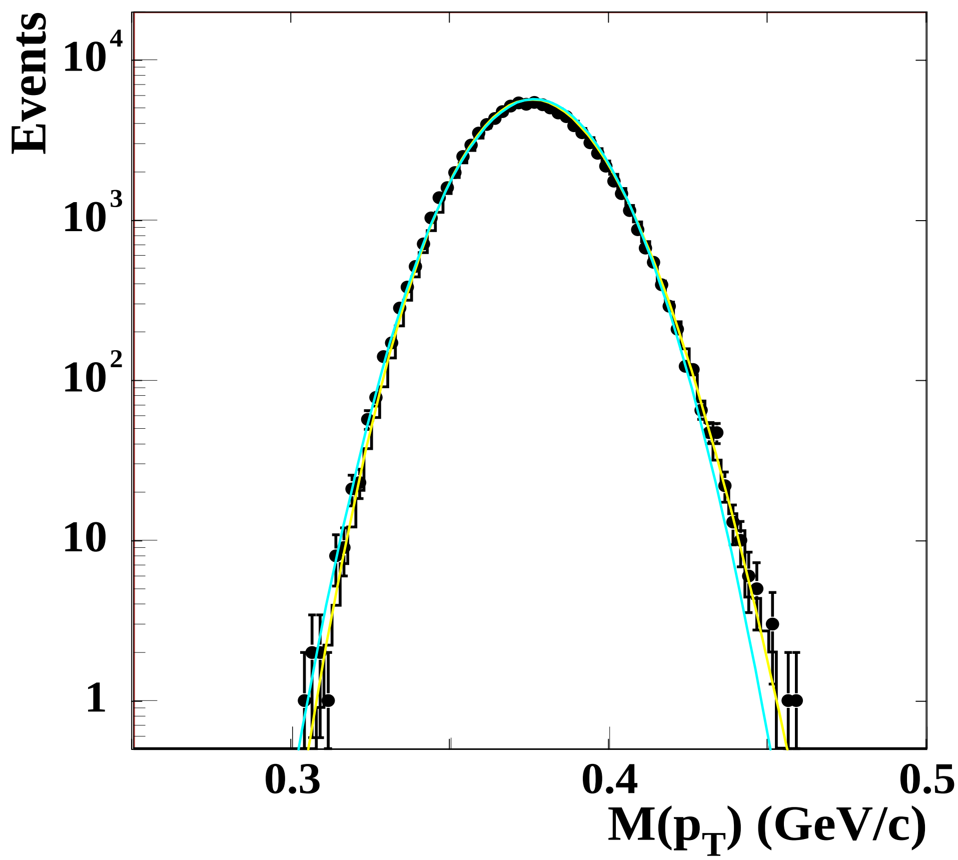

Figure 25: Full distribution in M_{p_T} (light line) compared to NA49 measurement (filled points) and mixed event distribution (histogram).

Hint, it's a Gamma Distribution
see M. J. Tannenbaum, Phys. Lett. B498, 29 (2001)

Event by Event Physics—RHIC results

STAR showed M_{p_T} at Quark Matter but

PHENIX Jeff Mitchell, APS Meeting April, Oct 2001

M_{p_T} and M_{E_T} vs Centrality
Anything beyond Statistical Independent Emission is Small $\sim$%

Charge Fluctuations Soon

Pion Interferometry—2-Particle Correlations

STAR π^- pairs $|\eta| < 0.5$, subm PRL May 2001
PHENIX, nucl-ex/0104020 (agrees with STAR, not shown)

$$C(q_1, q_2) = \frac{P(q_1, q_2)}{P(q_1)P(q_2)} = 1 + \lambda \exp(-Q_{inv}^2 R_{inv}^2)$$

$$C(q_1, q_2) = 1 + \lambda \exp(-R_o^2 q_{out}^2 - R_s^2 q_{side}^2 - R_l^2 q_{long}^2)$$

$C(Q)$ w/wo Coulomb

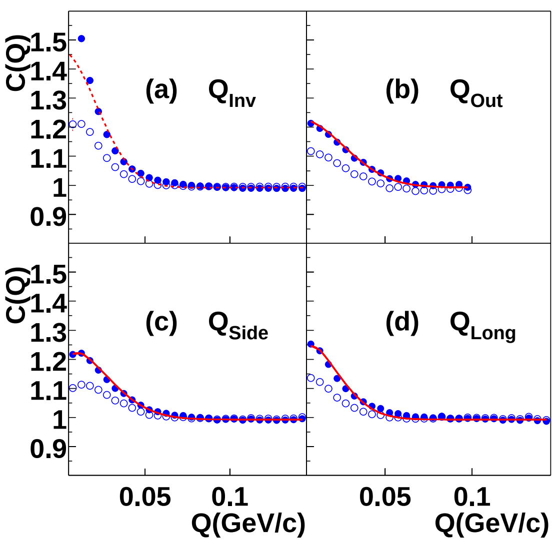

Central 12%. $0.125 < p_T < 0.225$ GeV/c

Centrality & m_T

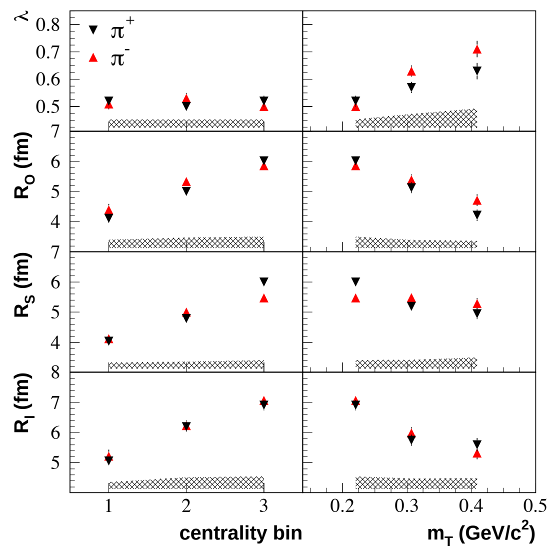

Bin 3 central 12%, bin 2 32%-12%, bin 1 62%-32% ($0.125 < p_T < 0.225$)

m_T for central

n.b. at $m_T = 0.4$ GeV/c^2 $R_o < R_s$
but conventionally the freezout duration $\tau = \sqrt{R_o^2 - R_s^2}/\langle\beta_T\rangle$?
THEORISTS start thinking

Midrapidity HBT Radii

$\sqrt{s_{NN}}$ dependence

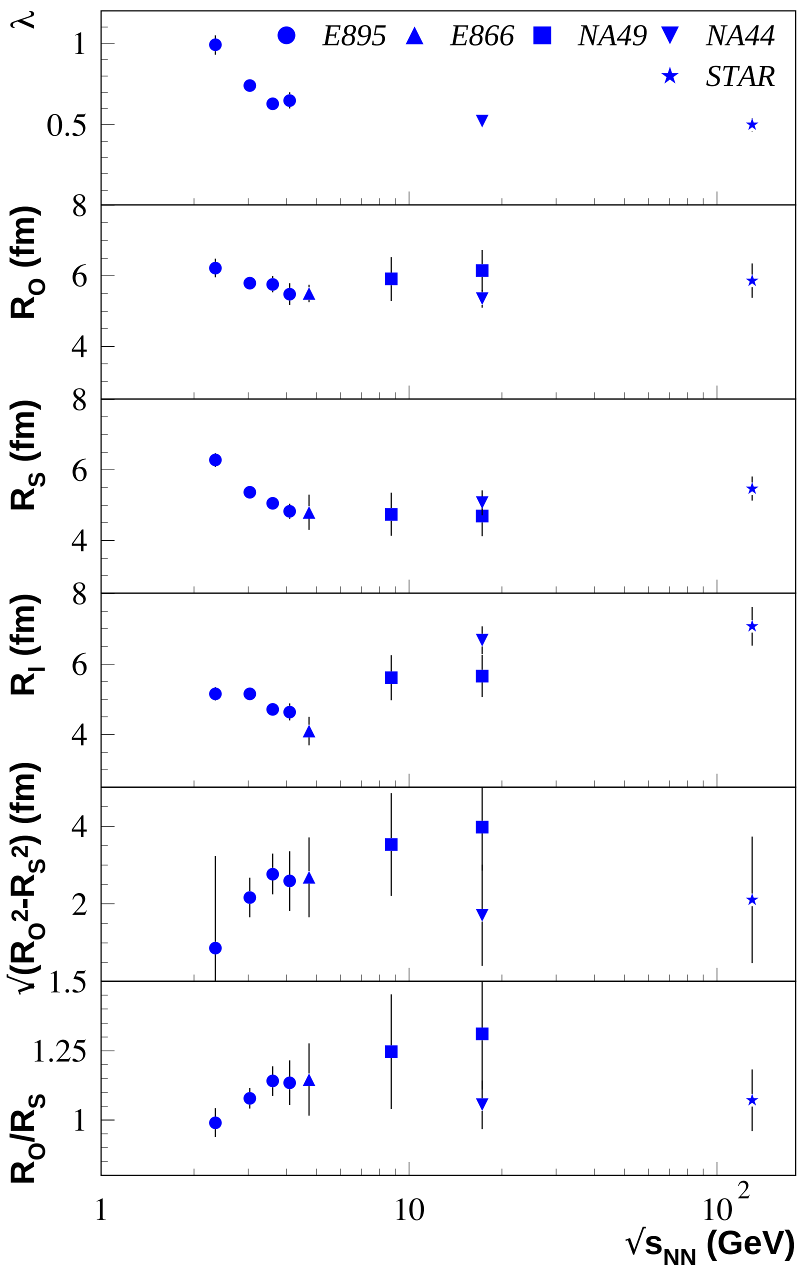

π^- HBT radii central Au+Au, Pb+Pb

Smooth continuation from lower energies, no anomalous sizes

Flow

Collective (not thermal) motion of particles outwards

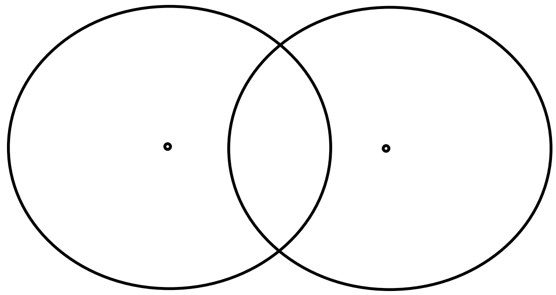

Flow comes in at least 3 different varieties.

• **Directed Flow—low energy:** At low energies, $E \leq 1$ A GeV, where there is very little particle production, the participating nucleons all scatter away from other the nucleus due to the high nuclear compressibility. This results in a scattering plane with an anisotropic particle distribution such that e.g. all participants move to the left in the projectile region and to the right in the target region. Also, the slow moving spectators block the produced particles so that they 'squeeze' out perpendicular to the scattering plane.

• **'Elliptic' Flow:** At AGS energies, the spectators move faster and more particles are produced, so that for $E > 4$ A GeV there is a transition to where particles are produced dominantly in the production plane outwards from the 'almond'. This 'elliptic' flow is left-right symmetric, and gives a $\cos(2\phi)$ distribution of particles azimuthally around the reaction plane.

• **Radial or Transverse Flow:** The two 'anisotropic' flows vanish for central collisions, where yet another type of flow, called transverse or radial, occurs. This is thought to be the cause of the increase of $\langle m_T - m_o \rangle$ with particle mass shown in Fig. 8.

Azimuthal Anisotropy

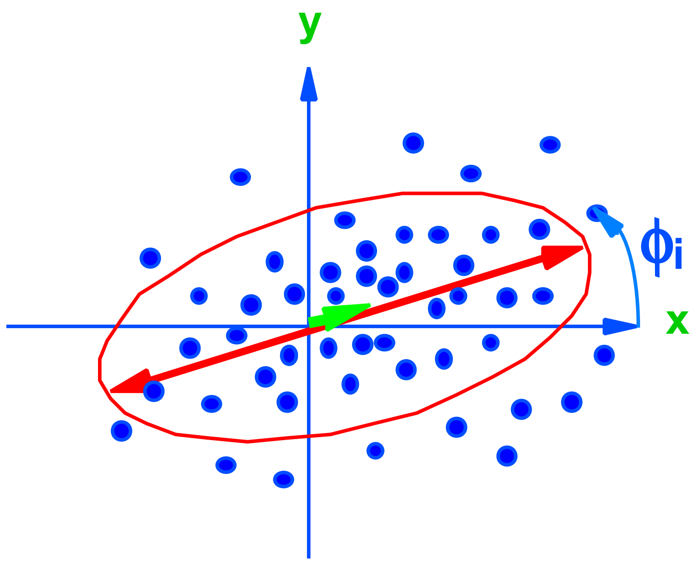

- **Find event plane**

$$\Psi_2 = \frac{1}{2}\tan^{-1}\left(\frac{\sum_i w_i \cdot \sin(2\phi_i)}{\sum_i w_i \cdot \cos(2\phi_i)}\right)$$

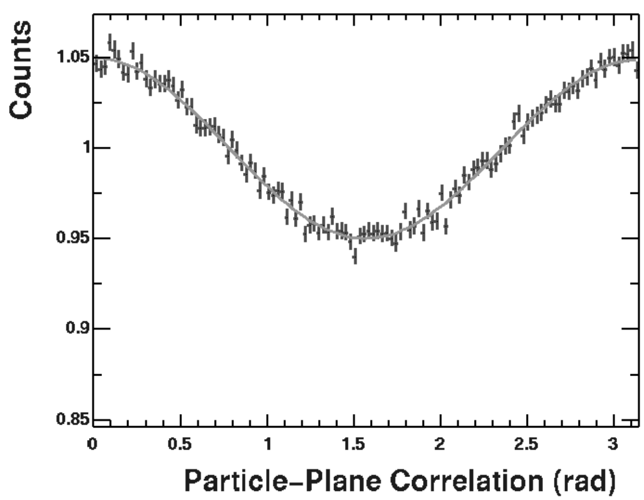

- **Correlate particles to event plane**

$$v_2 = \langle \cos(2[\phi - \Psi_2]) \rangle$$

•**PRL 86:402, 2001**

Elliptic Flow—Star

Phys. Rev. Lett. **86**, 402 (2001), nucl-ex/0104006

The 'Almond'

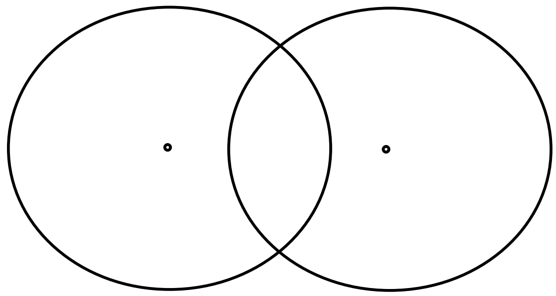

v_2 vs Centrality

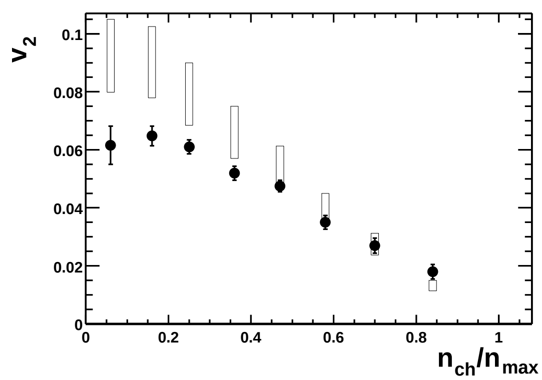

Elliptic Flow vs Almond ϵ

v_2 vs p_T

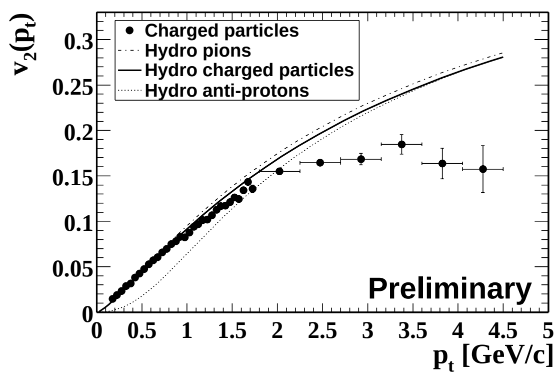

MinBias, all charged particles

peak v_2 vs $\sqrt{s_{NN}}$

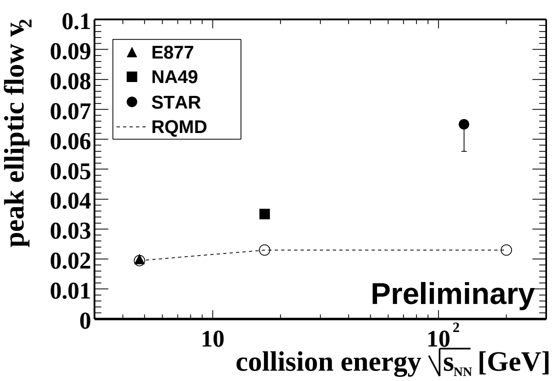

peak v_2 from AGS to RHIC

PHOBOS nucl-ex/0105015

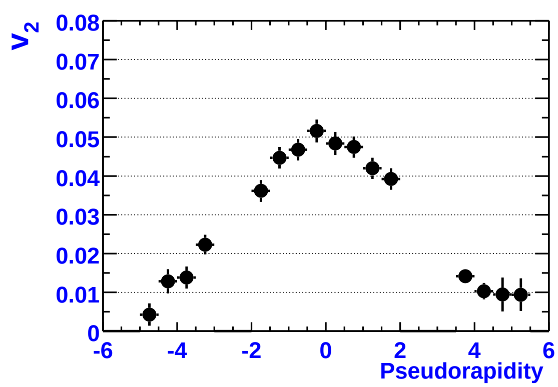

PHOBOS v_2 vs η MinBias

Elliptic Flow—PHENIX

Uses 2-particle Azimuthal Correlations nucl-ex/0105003

Uses standard 2-particle Correlation Function

$$C(\Delta\phi) = \frac{F_{cor}(\Delta\phi)}{B_{uncor}(\Delta\phi)}$$

$$C(\Delta\phi) \propto [1 + 2\lambda_1 \cos(\Delta\phi) + 2\lambda_2 \cos(2\Delta\phi)]$$

$$v_2 = \sqrt{\lambda_2}$$

$F_{cor}(\Delta\phi)$ $B_{uncor}(\Delta\phi)$ $C(\Delta\phi) = F/B$

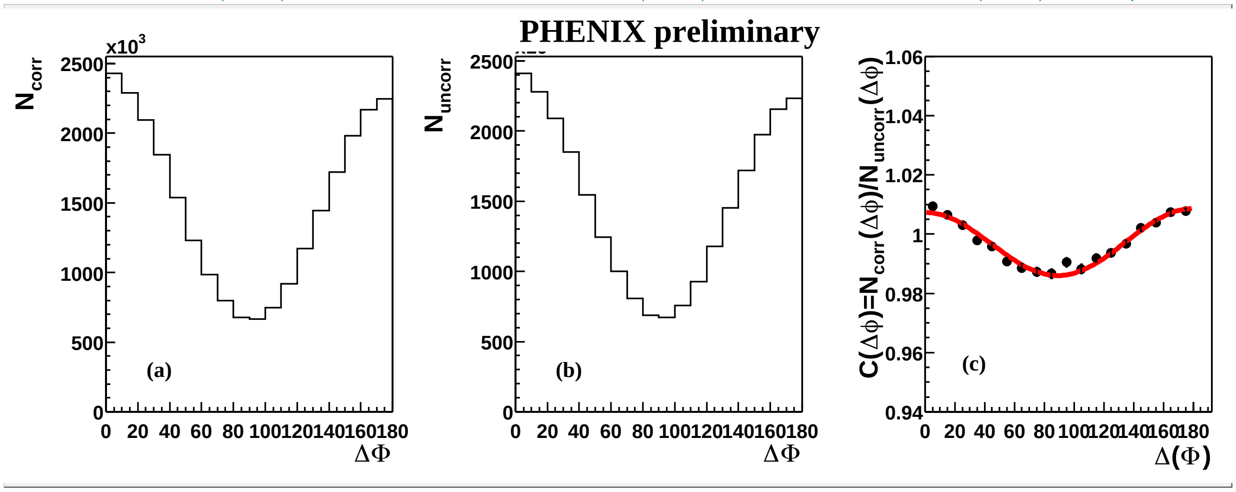

New Elegant Theoretical Analysis
N. Borghini, P. M. Dinh, J.-Y. Ollitrault, nucl-th/0105040

STAR Resonances, Hyperons, Antinucleons

nucl-ex/0104001, nucl-ex/0104007

$\Lambda\ \bar{\Lambda}$

$\phi \rightarrow K^+K^-$

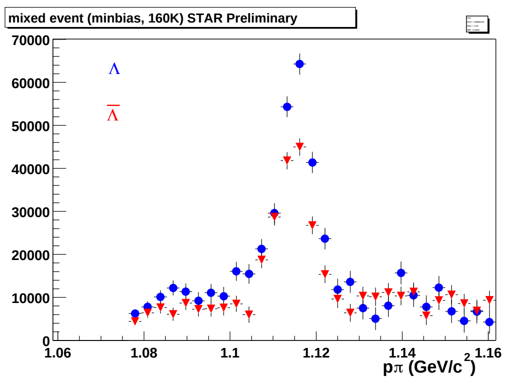

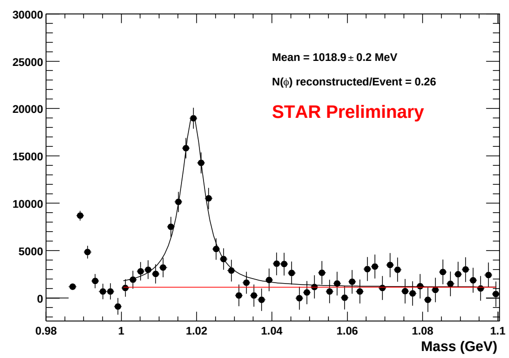

$\bar{\Lambda}/\Lambda = 0.73 \pm 0.03\ p_T < 2$ GeV/c

$K^{*0} \rightarrow K^+ + \pi^-$

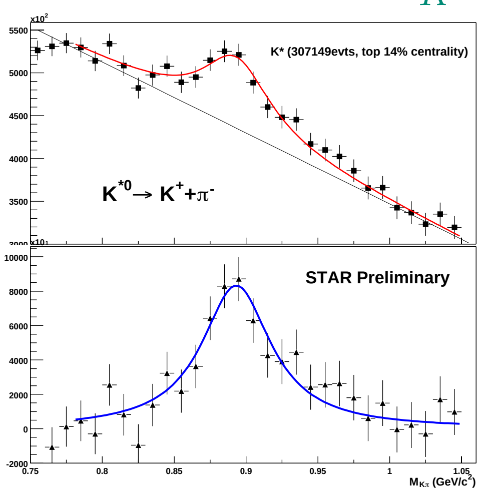

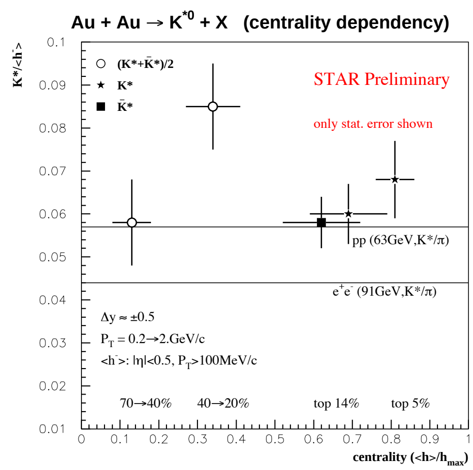

$K^{*0}/h^- \approx 0.07\ K^{*0}/K \approx 0.4 \sim 25\%$ systematic errors

Factor of 50 increase of $\bar{d}$ cf CERN SPS

Single $e^{\pm}$, e^+e^- pairs—PHENIX

PHENIX qm01, Y. Akiba,

`http://www.phenix/bnl.gov/phenix/WWW/publish/akiba/QM2001/proceeding/`

$\pi^{\pm}$, π^0, h^-, $e^{\pm}$

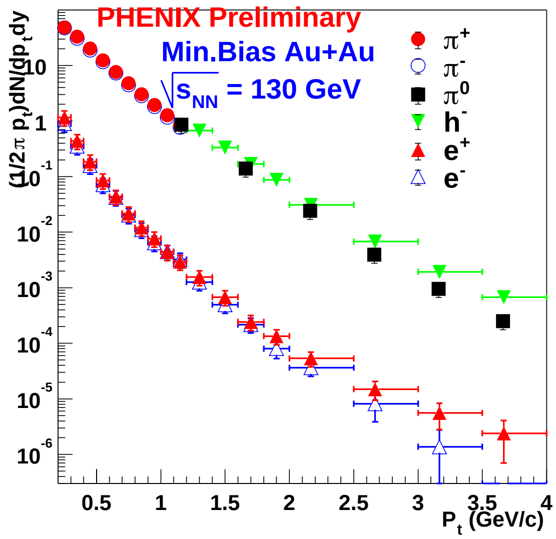

Photons from conversions

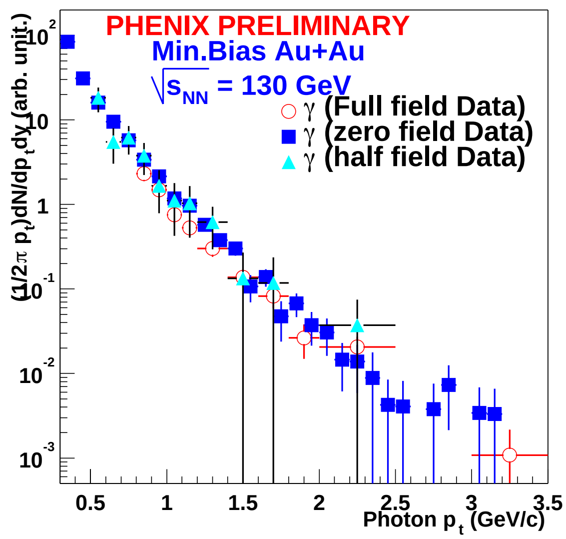

e^+e^- **Pairs (3** J/Ψ **??)**

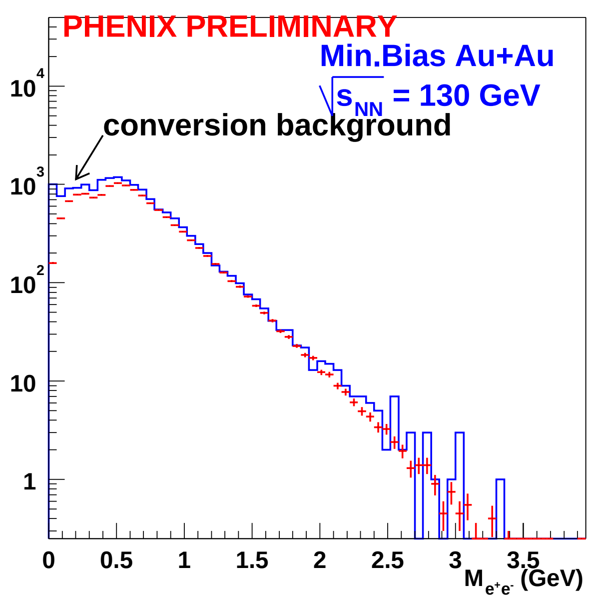

Signal (blue) c.f. mixed events (red)

Nothing Dramatic with single e **or photon**

Next year ~ 10000 $J/\Psi \to \mu^+\mu^-$, ~ 2000 e^+e^-